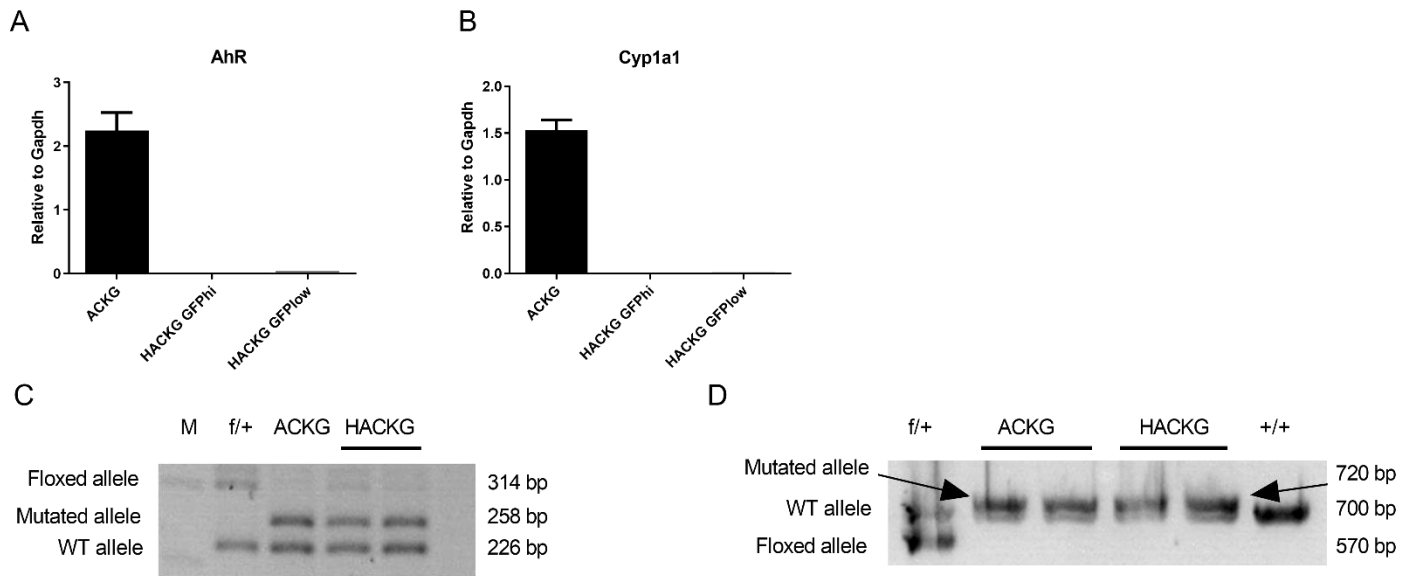
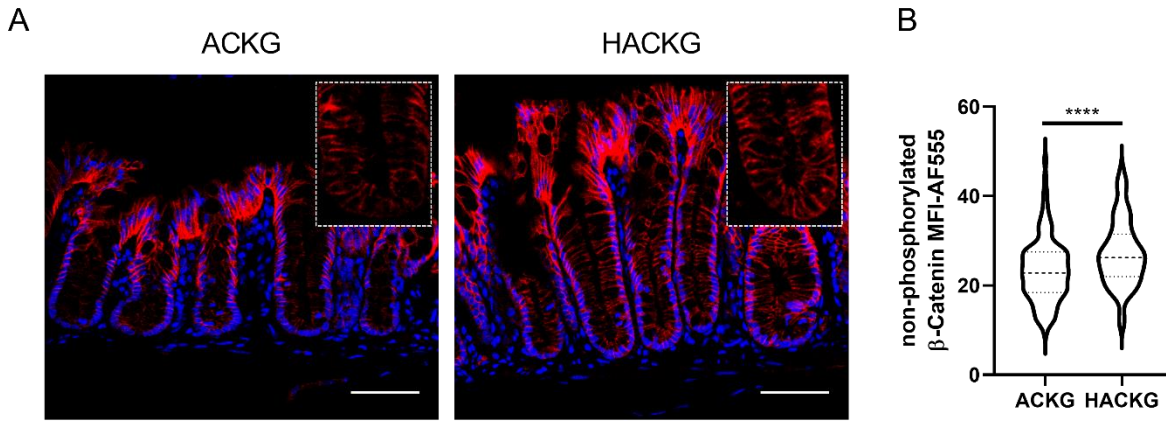


## Supplemental Figures



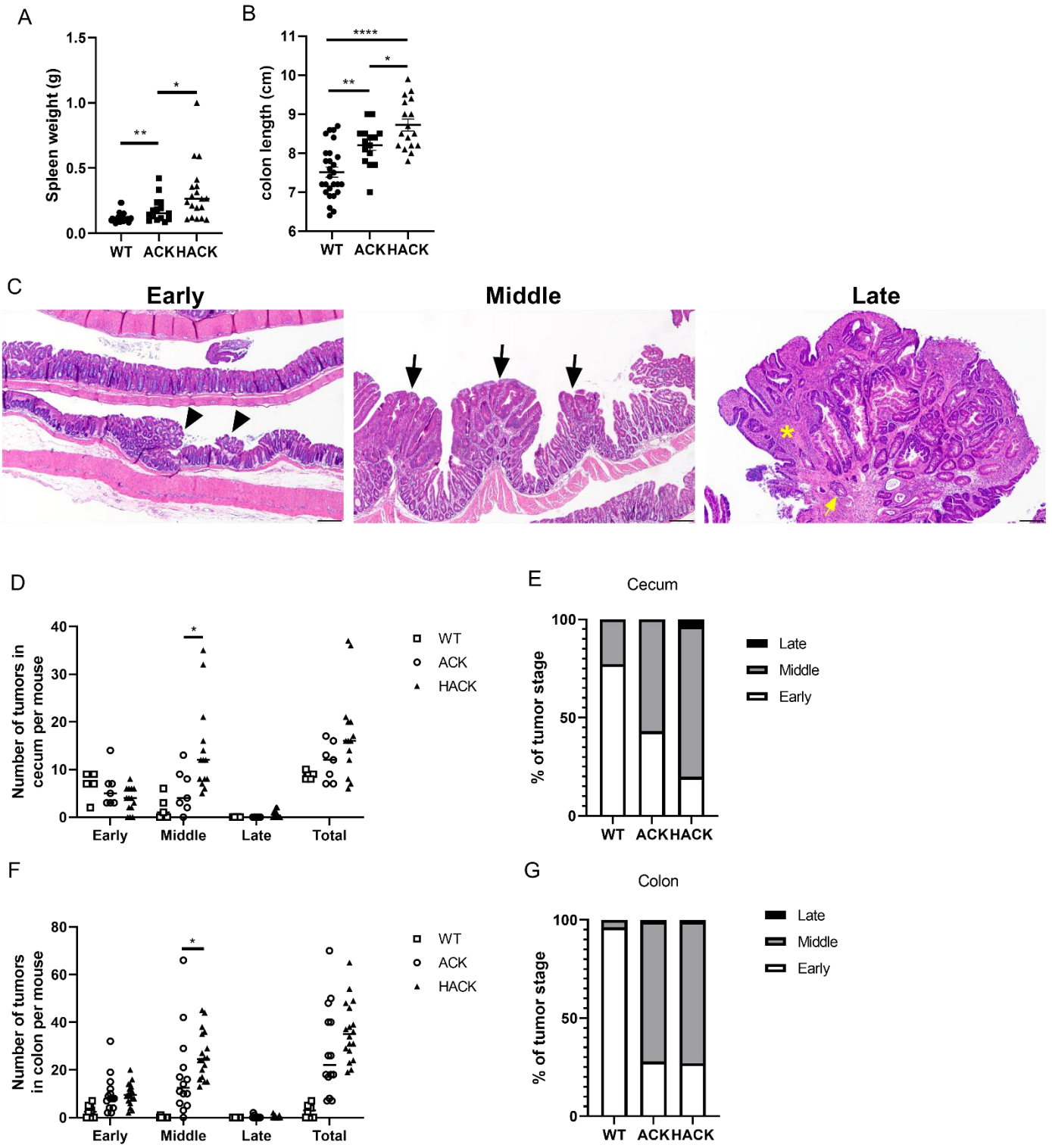
### Supplemental Figure 1

**Supplemental Figure 1.** Characterization of genotypes. (A-B) Expression of AhR and Cyp1a1 in organoids derived from sorted stem cells in ACKG and HACKG mice, n=2 per group. Data are presented as mean  $\pm$  SEM. (C-D) PCR genotyping analysis of (C) Apc and (D) Kras in organoids derived from sorted stem cells in ACKG and HACKG mice. f: floxed allele; +: WT allele. See methods section for additional details.



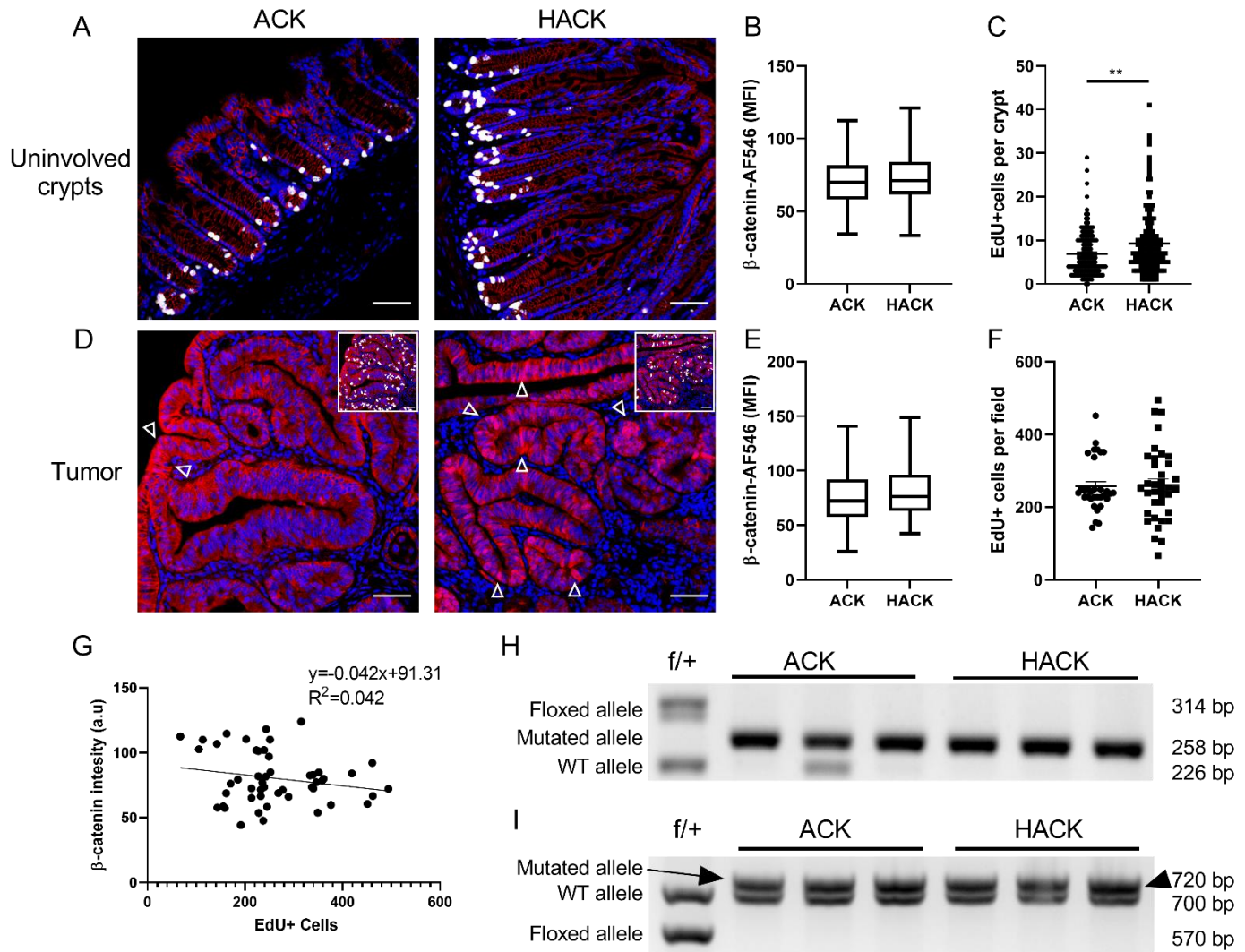
### Supplemental Figure 2

**Supplemental Figure 2.** Loss of AhR increases non-phosphorylated  $\beta$ -catenin. Mice were administered tamoxifen for 4 consecutive days and terminated 3 wk post the final tamoxifen injection. (A) Representative immunohistochemistry of non-phosphorylated (active)  $\beta$ -catenin in the distal colon of ACKG and HACKG mice. Scale 50  $\mu$ m. The inset showed the magnified presentation of active  $\beta$ -catenin. Blue, DAPI; Red, active  $\beta$ -catenin. (B) Quantification of MFI of non-phosphorylated  $\beta$ -catenin in lower crypt regions, n=118-125 crypts from 4 mice per group. \*\*\*\*p<0.0001.



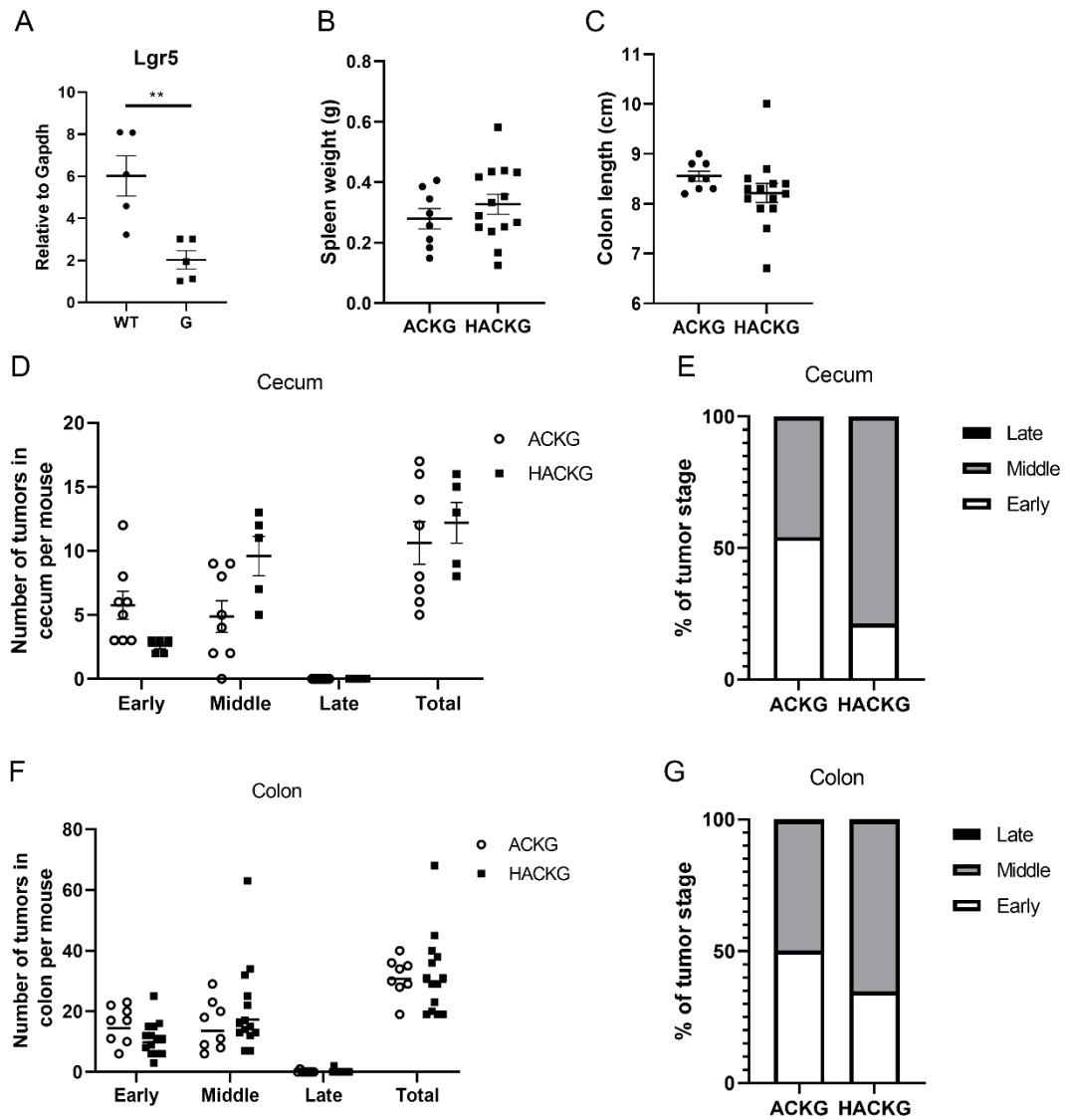
**Supplemental Figure 3**

**Supplemental Figure 3.** Intestinal pathology analysis from ACK and HACK mice. (A) Spleen weight, n=15-27 mice per group. (B) Colon length, n=15-27 mice per group. (C) Representative H&E staining of early, mid, and late stage lesions from the colon. Early lesions exhibited mucosal hyperplasia (arrowheads). Mid-stage lesions included foci of adenomatous hyperplasia (arrows). Late stage lesions had progressed to adenocarcinoma of the colonic epithelium with invasion into the submucosa (yellow arrow). Neoplastic cells were embedded in a proliferative fibrovascular stroma (yellow asterisk). Scale bar, 200  $\mu$ m. (D) The number of scored cecal tumors per mouse. (E) Analysis of tumor stage in cecal tumors. (F) The number of scored colonic tumors per mouse. (G) Analysis of tumor stage in colon tumors. Quantitative scores in (D-G) were based on H&E sections from each mouse, n=5-14 mice per group. \*p<0.05, \*\*p<0.01, \*\*\*\*p<0.0001.



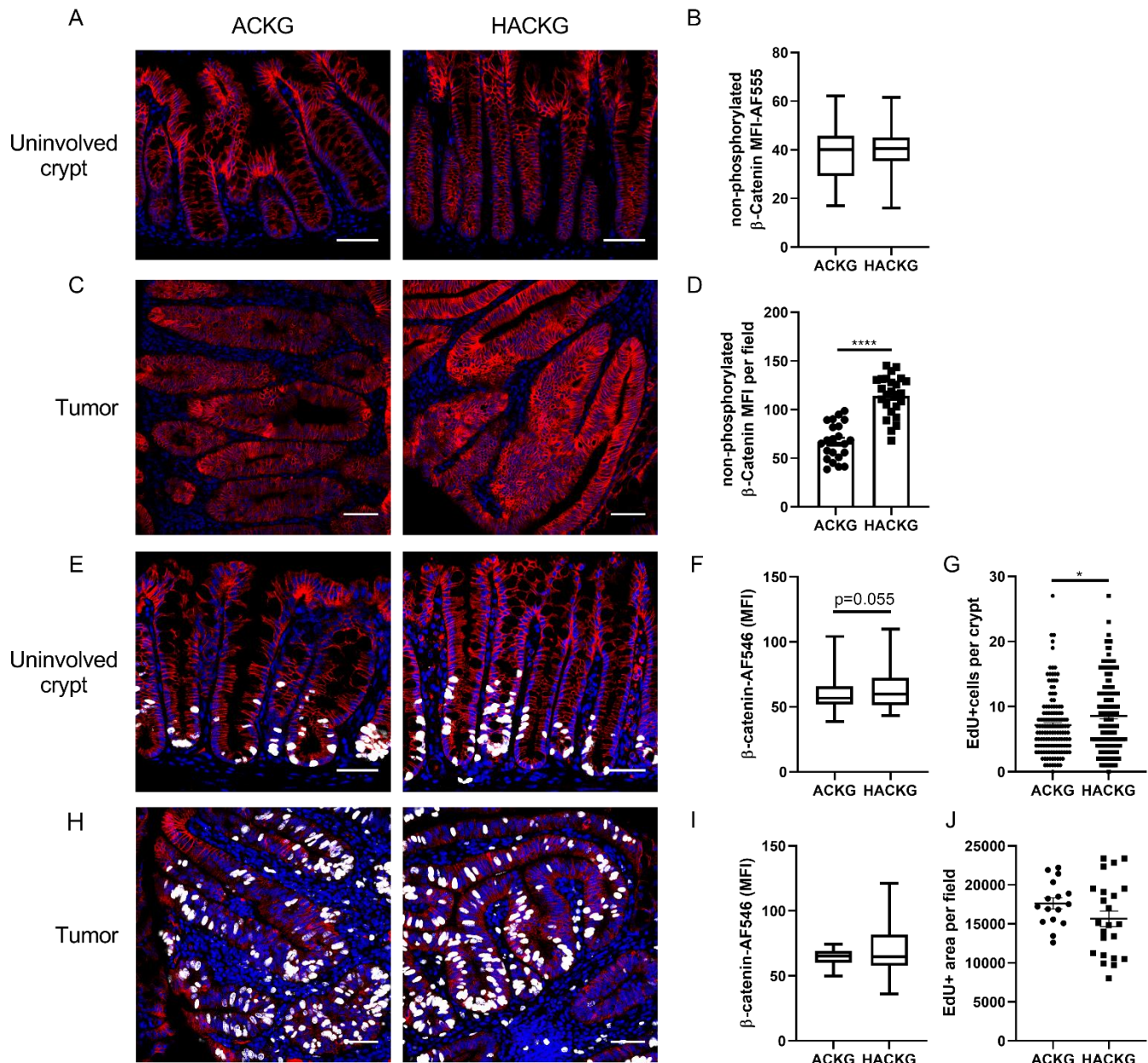
**Supplemental Figure 4**

**Supplemental Figure 4.** AhR deletion promotes cell proliferation. (A) Total  $\beta$ -catenin and cell proliferation marked by EdU<sup>+</sup> cells in the uninvolved distal colon of ACK and HACK mice. Blue, DAPI; Red,  $\beta$ -catenin; and Gray, EdU. Scale bar, 50  $\mu$ m. (B) Quantification of MFI of  $\beta$ -catenin per crypt and (C) EdU<sup>+</sup> cells per crypt. Each dot represents one crypt from n=4 mice per group. (D) Total  $\beta$ -catenin and cell proliferation marked by EdU<sup>+</sup> cells in colonic tumors from ACK and HACK mice. Blue, DAPI; Red,  $\beta$ -catenin; and Gray, EdU. Scale bar, 50  $\mu$ m. Arrow denotes accumulation of nuclear  $\beta$ -catenin. Quantification of MFI of (E)  $\beta$ -catenin per crypt and (F) EdU<sup>+</sup> cells per crypt, n=4 mice per group. (G) The association between MFI of  $\beta$ -catenin and EdU<sup>+</sup> cells. Each dot represents different image fields from n=4 mice. (H-I) PCR genotyping analysis of (H) *Apc* and (I) *Kras* in organoids from proximal colon tumors with diameter greater than 5 mm. f: floxed allele; +: WT allele. Organoids were cultured in medium without EGF, Wnt3a and R-Spondin growth factors.



**Supplemental Figure 5**

**Supplemental Figure 5.** Intestinal pathology analysis from ACKG and HACKG mice. (A) Reduced Lgr5 expression in Lgr5-GFP reporter (G) mice, compared with WT (no mutations) mice, n=5 mice per group. (B) Spleen weight, n=8-14 mice per group. (C) Colon length, n=8-14 mice per group. (D) The number of scored cecal tumors per mouse. (E) Analysis of tumor stage in cecal tumors. (F) The number of scored colonic tumors per mouse. (G) Analysis of tumor stage in colon tumors. Quantitative scores in (D-G) were based on H&E sections from each mouse, n=5-14 mice per group. \*\*p<0.01.



**Supplemental Figure 6**

**Supplemental Figure 6.** Wnt signaling in Lgr5 haploinsufficient mice. (A) Representative immunohistochemistry of non-phosphorylated (active)  $\beta$ -catenin in tumor uninvolved tissues. Scale 50  $\mu$ m. (B) Quantification of MFI of non-phosphorylated  $\beta$ -catenin in lower crypt regions,  $n=138$ -160 crypts from 4-5 mice per group. (C) Representative immunohistochemistry of non-phosphorylated (active)  $\beta$ -catenin in colonic tumor tissues. Scale 50  $\mu$ m. (D) Quantification of MFI of non-phosphorylated  $\beta$ -catenin per field,  $n=22$ -25 fields from 3-4 mice per group. (E) Representative fluorescent images of total  $\beta$ -catenin and cell proliferation in the uninvolved distal colon of ACKG and HACKG mice. Blue, DAPI; Red,  $\beta$ -catenin; and Gray, EdU. Scale bar, 50  $\mu$ m. (F) Quantification of MFI of total  $\beta$ -catenin per crypt and (G) EdU<sup>+</sup> cells per crypt,  $n=4$  mice per group. (H) Representative fluorescence images of total  $\beta$ -catenin and cell proliferation in colonic tumors from ACKG and HACKG mice. Blue, DAPI; Red,  $\beta$ -catenin; and Gray, EdU. Scale bar, 50  $\mu$ m. (I) Quantification of MFI of total  $\beta$ -catenin per crypt and (J) EdU<sup>+</sup> cells per crypt,  $n=4$  mice per group. \* $p<0.05$ , \*\*\*\* $p<0.0001$ .